

# Simultaneous detection of multiple charged particles using a borosilicate nanopore-based sensor

Yuqian Zhang *Student Member, IEEE*, Leyla Esfandiari\* *Member, IEEE*,

**Abstract**— Nanopore sensing has been widely researched owing to its single molecule sensitivity. In this work, we have demonstrated the potential application of a relatively low-cost single borosilicate nanopore-based sensor for simultaneous detection of multiple charged particles with various diameters.

**Keywords**— Nanopore sensing, multiplex, carboxylate beads, nucleic acids.

## I. INTRODUCTION

The field of nanopore-based sensing was inspired by the well-known Coulter Counter device [1, 2], in which macromolecules are driven through a pore with small diameter by applied pressure or electrical field. As each molecule passes through the pore, the change in pore's conductance is measured as a unique electrical pulse to the macromolecule's physical size and geometry. Thus, various molecules could simultaneously be detected at a very low concentration [3].

In past two decades, biological and solid-state nanopores have gained significant attention in the field of genome sequencing [4-6]. However, the low temporal resolution of single nucleotide detection, as a nucleic acid molecule travels through the pore has partially changed the nanopore's application from sequencing to sensing [7-9]. For instance, Kasianowicz et al., has demonstrated the detection of two different proteins using an embedded  $\alpha$ -hemolysin ( $\alpha$ HL) pore in an artificial lipid bilayer platform [10]. In another study by Wanunu et al., small nucleic acids, 25-bp DNA, 22-bp RNA, and tRNA were discriminated using a 3-nm-diameter pore in a 7-nm-thick silicon nitride (SiN) membrane [11]. Additionally, two different antibodies were detected utilizing a single outer membrane protein G (OmpG) nanopore in an artificial lipid bilayer platform by Chen group [12]. Rotem et al. showed the application of an  $\alpha$ HL pore modified with a 15-mer DNA aptamer to quantify concentration of thrombin [13]. Moreover, Wei et al. modified metallized SiN nanopore with nitrilotriacetic acid receptors to detect His-tagged proteins [14]. The majority of approaches described above are required to integrate with a high resolution amplifier in order to detect the small changes (pico to nano Amps) in ionic current. However, the addition

of a high resolution amplifier such as Axopatch 200B adds bulk and cost to the detection platform.

In order to omit the Axopatch amplifier, our group, Esfandiari et al, has previously demonstrated the binary-mode (yes/no) detection of sequence-specific DNA with single base mismatch specificity at an impressive concentration detection limit of 10fM utilizing a borosilicate pore and electrostatically neutral peptide nucleic acid (PNA) probes conjugated to polystyrene beads [15, 16]. In this method the probe conjugated polystyrene bead is utilized as an intrinsic mechanical amplifier; this intrinsic mechanical amplifier combined with a simple inverting op-amp enhance the current signal to easily detectable micro-Amp range. Thus, the developed detection module simplifies the device electronics and the measurement readouts and thus has the potential to be used as a robust and low-cost molecular sensor.

Here, we take the single analyte detection concept a step further to demonstrate the feasibility of the nanopore-based platform as a cost-effective multiplex sensor. Utilizing this detection method, multiple analytes could be simultaneously and rapidly discriminated by carboxylate polystyrene beads with various diameters, as probe-substrate modules, in a single nanopore-based sensing scheme (Figure 1). In this study the proof of concept has been demonstrated by easily measuring the changes in ionic current as beads with different diameters block or pass through a single pore. The measured data were simply interpreted and supported by a mathematical model.

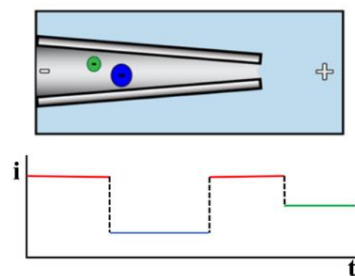


Figure 1. Schematic illustration of multiplexing concept in a single nanopore using two beads with different diameters.

## II. PROCEDURE

### A. Materials

Potassium chloride, HEPES, and sodium hydroxide were purchased from Sigma-Aldrich (St. Louis, MO). Silicone elastomer base and silicone elastomer curing agent were obtained from Dow Corning (Elizabethtown, KY). Fluorescently tagged, carboxylic acid-functionalized polystyrene, carboxylic acid-functionalized polystyrene

\* Corresponding authors

Yuqian Zhang and Ankit Rana are with the department of electrical and computing system, University of Cincinnati, Cincinnati OH.

Leyla Esfandiari is with the department of electrical and computing system, University of Cincinnati, Cincinnati OH, USA (corresponding author: 513-556-1355; e-mail: Leyla.esfandiari@uc.edu).

beads with  $0.97\mu\text{m}$ ,  $1.04\mu\text{m}$  and non-fluorescent carboxylic acid-functionalized beads with  $1\mu\text{m}$ ,  $2.36\mu\text{m}$  diameters were purchased from Bangs Laboratories, Inc. (Fishers, IN).  $1\mu\text{m}$  diameter pre-pulled borosilicate glass micropipettes were purchased from World Precision Instruments, Inc. (Sarasota, FL).

### B. Sensor Apparatus and Electrical Measurement

Polydimethylsiloxane (PDMS) molds were fabricated with  $1\text{mm}$  outer diameter cylinder opening between two chambers, and bonded with a glass slide via Oxygen Plasma Cleaning technique (March CS-170).  $1\mu\text{m}$  ( $\pm 20\%$ ) pre-pulled borosilicate pore was inserted into opening cylinder and sealed with vacuum grease so that the pore was the only connection between the two reservoirs. Micropipette was back filled with electrolyte ( $1\text{mM}$  KCl and  $10\text{mM}$  HEPES, pH 7.0) with a 33 gage Hamilton syringe needle, and two reservoirs were filled with buffer as well.

Platinum electrodes were placed into two reservoirs and  $30\text{V}$  DC potential difference was applied using Keithley 2220G-30-1 voltage generator. The ionic current output was amplified with a trans-impedance amplifier (OPA 111). The signal was digitized by acquisition hardware at  $1\text{kHz}$  (USB 6361, National Instruments) and recorded with LabVIEW software (National Instruments). Prior to injection of the beads the baseline current was recorded.  $1\mu\text{L}$  carboxylate beads were diluted in  $1\text{mL}$  buffer and injected into the pore. Negatively charged beads were electrophoretically mobile and were monitored using an inverted fluorescent microscope, Nikon Eclipse TE2000-E equipped with a high resolution camera Andor NeoZyla 5.5 with  $100\text{ frames/sec}$  capturing frequency.

## III. RESULTS AND DISCUSSION

To investigate the multiplexing capability of the system, negatively charged carboxylate beads with different diameters were used. Our hypothesis is that since the detection scheme depends on the electrostatic charge of the target analytes [16], negatively charged carboxylate beads are desirable to illustrate the feasibility of multiplexing with various sizes. Figure 2 illustrates the microscopic image of two type of carboxylate beads (fluorescent and non-fluorescent) with two different diameters traveling toward the pore under the applied electric field. The diameter of

each bead and thus its corresponding unique current pulse is the key element of the multiplex sensing concept in order to simultaneously detect various analytes by the probe-conjugated beads.

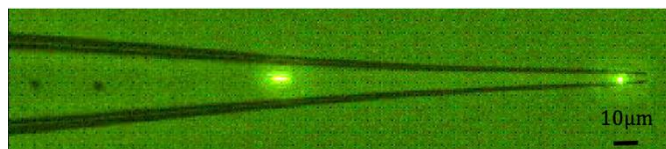


Figure 2. Microscope image of two different sizes of carboxylate beads travelling towards a pore under the electric field.

We have chosen a pre-pulled glass as a nanopore sensor in order to take advantage of the transparency criteria of the glass pore mounted on the PDMS/glass substrate for real-time microscopic visualization purpose. Also, pre-pulled glass nanopores have been used as an attractive simple and cost effective device for molecular sensing by other research groups [17-21]. A study by Keyser group has demonstrated a cost-effective method for the simultaneous sensing of molecules using sixteen pre-pulled glass pores [22]. In this study, we even simplify the device and its cost further by demonstrating the multiplex sensing capability using only a single glass pore.

Initially,  $1\mu\text{m}$  and  $2.36\mu\text{m}$  diameter carboxylate beads were injected into a  $1\mu\text{m}$  diameter borosilicate pore and the conductance across the pore was measured as describe previously [15, 16]. Beads were driven by the electrophoretic force which moved towards the lower potential and therefore blocked the pore. As a result, the resistance across the pore increased immediately, causing the ionic current to drop. Pore was re-opened by reversing the applied potential and the ionic current recovered to its initial state; the pore blockades were repeatable. The ionic current pulses corresponding to passage of beads were analyzed and confirmed by matching the electrical signal's time stamp to the corresponding microscopic footage. The analysis was consistent for two population of beads with different diameters as shown in Figure 3. In case of  $1\mu\text{m}$  diameter beads (Figure 3a), the average percentage of current blockade was  $3.56\% \pm 0.0045$ . In case of  $2.36\mu\text{m}$  (Figure 3b), the average percentage of current blockade was  $19.77\% \pm 0.0061$  and the pore blocks

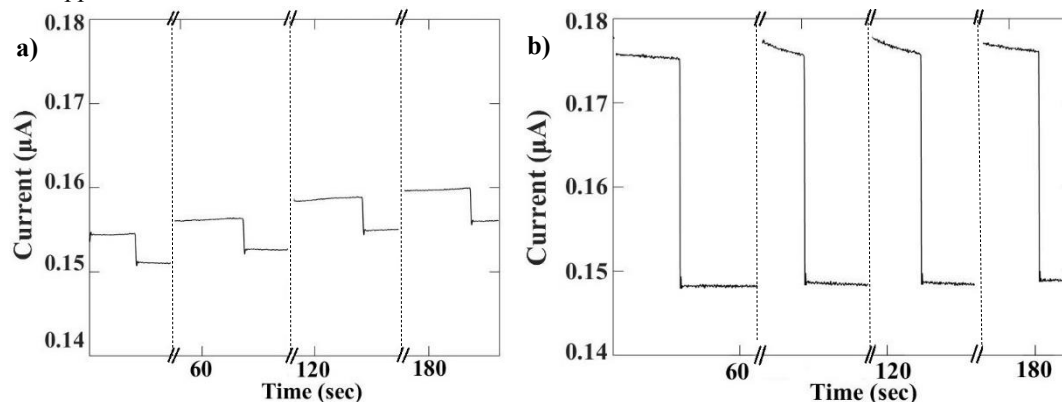


Figure 3. Illustrates ionic current drop of two population of beads with different radii a) 4 ionic current drops caused by  $1\mu\text{m}$  diameter carboxylic-acid-functionalized beads blocking a  $1\mu\text{m}$  diameter pore. The blockades are reversable and repeatable. b) 4 ionic current drops caused by  $2.36\mu\text{m}$  diameter carboxylic-acid-functionalized beads blocking a  $1\mu\text{m}$  diameter pore. The blockades are reversable and repeatable.

were repeated 21 times (data not shown). The average ionic current blockades of the two population of beads were significantly different from one another which demonstrates the feasibility of multiplex sensing of the device by two population of beads with different hydrodynamic radii.

In another experiment, a mixture of 0.97 $\mu\text{m}$  fluorescent beads (emitting green light) and 1.04 $\mu\text{m}$  fluorescent beads (emitting blue light) were injected into the 1 $\mu\text{m}$  pore. The pore diameter appeared to be larger than 1 $\mu\text{m}$  since the 1.04  $\mu\text{m}$  beads could pass through the pore (observed microscopically). Both microsphere populations could pass through the pore which caused transient blockades with significantly differentiable pulses as shown in Figure 4. Figure 4a. illustrates seven translocation events recorded in 2 minutes which were associated and confirmed with microscopic footage. Two pulses were detected with larger decrease in ionic current amplitude (pulse #4 and #7) which were the result of 1.04 $\mu\text{m}$  diameter beads passing through the pore while the other five pulses were corresponded with translocation of 0.97 $\mu\text{m}$  beads. Empirical resistance increase of 8.66 M $\Omega$  was calculated (Applied Voltage divided by the measured current) for 1.04 $\mu\text{m}$  beads' passage and 4.8M $\Omega$  was calculated for 0.97 $\mu\text{m}$ . The average percentage of resistance increase for 1.04 $\mu\text{m}$  diameter beads was 5.23% $\pm$ 0.0053 while the average resistance changes was 2.2% $\pm$ 0.0029 for 0.97 $\mu\text{m}$  beads.

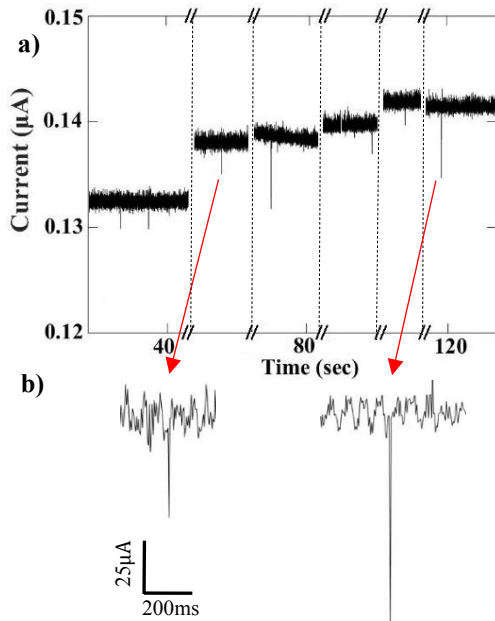


Figure 4. a) Resistive pulses of 0.97 $\mu\text{m}$  and 1.04 $\mu\text{m}$  diameter carboxylic-acid-functionalized beads passing through a 1 $\mu\text{m}$  diameter pore. b) Zoom in image of pulses (red arrows) of 0.97 $\mu\text{m}$  (left) and 1.04 $\mu\text{m}$  (right) beads.

Based on the resistive pulse measurements in this study, we have illustrated that the ratio of the hydrodynamic radius of beads to the pore diameter plays a key role in the multiplexing capability of the sensor. In order to confirm our empirical results, we have used the Gregg and Steidley's mathematical model [23], regarding the size of resistive pulses in a cylindrical channel and expanded the theoretical expression in a conical channel as described previously [15].

In this deviation, microspheres were treated as dielectric, neglecting their capacity effects. Figure 5 represents the schematic of the parameters that were used in this model. The resistance of conical channel with a particle inside derived in equation (1).

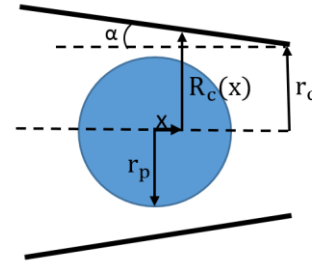


Figure 5. Schematic of the mathematical model used to approximate the micropipette geometry.

$$dR(x) = \frac{\rho dx}{A(x)} = \frac{\rho dx}{\pi[R_c^2(x) - (r_p^2 - x^2)]}$$

$$= \frac{\rho dx}{\pi[(r_c - x \tan \alpha)^2 - (r_p^2 - x^2)]} \quad (1)$$

Where  $\rho$  is the solution resistivity,  $r_c$  is the radius of the micropipette at the position of the particle center, and  $r_p$  represents the radius of microsphere.  $\alpha$  is the half-angle of conical micropipette. We estimated  $\alpha = 5^\circ$  and  $r_c = 1.1\mu\text{m}$ .

Integrating  $x$  from  $-r_p$  to  $r_p$  to obtain the resistance change as a microsphere with radius of  $r_p$  passes through a pore, Equation (2).

$$\Delta R = \int_{-r_p}^{r_p} dR(x)$$

$$= \frac{\rho}{\pi r_c \sqrt{1 - \sec^2 \alpha \left(\frac{r_p}{r_c}\right)^2}} \left[ \tan^{-1} \frac{[\tan \alpha + \sec^2 \alpha \frac{r_p}{r_c}]}{\sqrt{1 - \sec^2 \alpha \left(\frac{r_p}{r_c}\right)^2}} \right. \\ \left. - \tan^{-1} \frac{[\tan \alpha - \sec^2 \alpha \frac{r_p}{r_c}]}{\sqrt{1 - \sec^2 \alpha \left(\frac{r_p}{r_c}\right)^2}} \right] - \frac{2\rho \left(\frac{r_p}{r_c}\right)}{\pi r_c \sqrt{1 - \tan^2 \alpha \left(\frac{r_p}{r_c}\right)^2}} \quad (2)$$

In case of 1.04 $\mu\text{m}$  microspheres, the theoretical resistance change was calculated as  $\Delta R_{1.04\mu\text{m}} = 8.8\text{M}\Omega$  and the corresponding experimental resistance change was calculated as  $\Delta R'_{1.04\mu\text{m}} = 8.66\text{M}\Omega$ .

For 0.97  $\mu\text{m}$  microspheres, the theoretical result for resistance change was  $\Delta R_{0.97\mu\text{m}} = 5.2\text{M}\Omega$ , and the experimental measurement was  $\Delta R'_{0.97\mu\text{m}} = 4.8\text{M}\Omega$ .

Based on our calculations and measurements, theoretical results matched with experimental measurements and the small variation could be due to a finite dielectric constant of

microspheres possessed, or the geometry of microsphere is not an absolute sphere as we estimated.

#### IV. CONCLUSION

Results above showed that our device has high sensitivity to detect four different sizes of microspheres and display distinguishable ionic changes using a low-cost setup. Resistive pulses were consistent with the size of the beads both by theoretical and empirical data. This study proposed the feasibility of multiplexing by a single nanopore sensor. In future work, essential nucleic acid biomarkers with various sequences could be simultaneously detected by the complementary probe molecules conjugated to beads with different diameters in a single pore. This study is the first step towards development of a cost-effective, highly sensitive and robust multiplexer sensor using a nanopore.

#### REFERENCES

- [1] H. E. Kubitschek, "Electronic Counting and Sizing of Bacteria". *Nature* 1958, 182(4630), pp. 234-235.
- [2] S. M. Bezrukov, "Ion channels as molecular Coulter counters to probe metabolite transport." *Journal of Membrane Biology*, 2000, 174(1), pp. 1-13.
- [3] J. Clerk Maxwell, "A Treatise on Electricity and Magnetism", 3rd ed., vol. 2. Oxford: Clarendon, 1892, pp. 68-73.
- [4] J. Hahn and M. L. Charles, "Direct ultrasensitive electrical detection of DNA and DNA sequence variations using nanowire nanosensors." *Nano letters*, 2004, 4(1), pp. 51-54.
- [5] D. Branton, D. W. Deamer, A. Marziali, H. Bayley, S. A. Benner, T. Butler and S. B. Iovanovich. The potential and challenges of nanopore sequencing. *Nature biotechnology*, 2008, 26(10), pp. 1146-1153.
- [6] C. Y. Zhang, H. C. Yeh, M. T. Kuroki, and T. H. Wang. "Single-quantum-dot-based DNA nanosensor". *Nature materials*, 2005, 4(11), pp. 826-831.
- [7] S. Carson and M. Wanunu "Challenges in DNA motion control and sequence readout using nanopore devices". *Nanotechnology*, 2015, 26(7), pp. 074004.
- [8] K. Mathwig, T. Albrecht, E.D. Goluch and L. Rassaie. "Challenges of Biomolecular Detection at the Nanoscale: Nanopores and Microelectrodes". *Analytical chemistry*, 2015, 87(11), pp.5470-5475.
- [9] S. Lindsay. "The promises and challenges of solid-state sequencing". *Nature nanotechnology*, 2016, 11(2), pp.109-111.
- [10] A. Aksimentiev and K. Schulten. "Imaging  $\alpha$ -hemolysin with molecular dynamics: ionic conductance, osmotic permeability, and the electrostatic potential map." *Biophysical journal* 2005, 88(6), pp. 3745-3761.
- [11] M. Wanunu, T. Dadosh, V. Ray, J. Jin, L. McReynolds, and M. Drndić. "Rapid electronic detection of probe-specific microRNAs using thin nanopore sensors." *Nature nanotechnology*, 2010, 5(11), pp. 807-814.
- [12] M. Chen, S. Khalid, M.S. Sansom and H. Bavelle. "Outer membrane protein G: Engineering a quiet pore for biosensing" *Proceedings of the National Academy of Sciences*, 2008, 105(17), pp.6272-6277.
- [13] D. Rotem, I. Javasinghe, M. Salichou and H. Bavelle. "Protein detection by nanopores equipped with aptamers". *Journal of the American Chemical Society*, 2012, 134(5), pp.2781-2787.
- [14] R. Wei, V. Gatterdam, R. Wieneke, R. Tampé, and U. Rant. Stochastic sensing of proteins with receptor-modified solid-state nanopores. *Nature nanotechnology*, 2012, 7(4), pp.257-263.
- [15] L. Esfandiari, G. M. Harold, and J. S. Jacob J. "Sequence-specific nucleic acid detection from binary pore conductance measurement." *Journal of the American Chemical Society*, 2012, 134(38), pp. 15880-15886.
- [16] L. Esfandiari, M. Lorenzini, G. Kocharyan, H.G. Monbouquette and J.J. Schmidt. "Sequence-Specific DNA Detection at 10 fM by Electromechanical Signal Transduction". *Analytical chemistry*, 2014, 86(19), pp.9638-9643.
- [17] M. Karhanek, J. T. Kemp, N. Pourmand, R.W. Davis, and C.D. Webb. "Single DNA molecule detection using nanopipettes and nanoparticles". *Nano letters*, 2005, 5(2), pp. 403-407.
- [18] Y. Fu, H. Tokuhisa and L. A. Baker. "Nanonore DNA sensors based on dendrimer-modified nanopipettes". *Chemical Communications*, 2009 (32), pp. 4877-4879.
- [19] S. Umehara, M. Karhanek, R. W. Davis and N. Pourmand. "Label-free biosensing with functionalized nanonipette probes" *Proceedings of the National Academy of Sciences*, 2009, 106(12), pp. 4611-4616.
- [20] N. A. Bell and U. F. Keyser. "Specific protein detection using designed DNA carriers and nanopores". *Journal of the American Chemical Society*, 2015, 137(5), pp. 2035-2041.
- [21] L. J. Steinbock, R. D. Bulushev, S. Krishnan, C. Raillon and A. Radenovic. "DNA translocation through low-noise glass nanopores". *ACS Nano*, 2013, 7(12), pp. 11255-11262.
- [22] N. A. Bell, V. V. Thacker, S. Hernández-Ainsa, M. E. Fuentes-Perez, F. Moreno-Herrero, T. Liedl, and U. F. Keyser. "Multiplexed ionic current sensing with glass nanopores". *Lab on a Chip*, 2013, 13(10), pp. 1859-1862.
- [23] E. C. Gregg and K. D. Steidley. "Electrical counting and sizing of mammalian cells in suspension". *Biophysical journal*, 1965, 5(4), pp. 393.